RESEARCH PAPER

# Oxygen in the air and oxygen dissolved in the floodwater both sustain growth of aquatic adventitious roots in rice

Chen Lin[1], Lucas León Peralta Ogorek[2], Ole Pedersen[2] and Margret Sauter[1,*] (iD)

[1] Plant Developmental Biology and Plant Physiology, University of Kiel, Am Botanischen Garten 5, D-24118 Kiel, Germany
[2] Freshwater Biological Laboratory, Department of Biology, University of Copenhagen, Denmark

* Correspondence: msauter@bot.uni-kiel.de

Editor: Ian Dodd, Lancaster University, UK

## Abstract

Flooding is an environmental stress that leads to a shortage of $O_2$ that can be detrimental for plants. When flooded, deepwater rice grow floating adventitious roots to replace the dysfunctional soil-borne root system, but the features that ensure $O_2$ supply and hence growth of aquatic roots have not been explored. We investigate the sources of $O_2$ in aquatic adventitious roots and relate aerenchyma and barriers for gas diffusion to local $O_2$ gradients, as measured by microsensor technology, to link $O_2$ distribution in distinct root zones to their anatomical features. The mature root part receives $O_2$ exclusively from the stem. It has aerenchyma that, together with suberin and lignin depositions at the water–root and cortex–stele interfaces, provides a path for longitudinal $O_2$ movement toward the tip. The root tip has no diffusion barriers and receives $O_2$ from the stem and floodwater, resulting in improved aeration of the root tip over mature tissues. Local formation of aerenchyma and diffusion barriers in the mature root channel $O_2$ towards the tip which also obtains $O_2$ from the floodwater. These features explain aeration of floating roots and their ability to grow under water.

**Keywords:** Adventitious root, aerenchyma, barrier to radial oxygen loss, deepwater rice, flooding, lignin, oxygen, suberin.

## Introduction

Flooding imposes restrictions on plant growth and development that lead to severe crop losses worldwide (Tarlock and Chizewer, 2016; Olson *et al.*, 2017; Chen *et al.*, 2018). Flooding results in a slow gas diffusion rate and reduced light, both impairing photosynthesis and respiration (Colmer and Pedersen, 2008). Roots are most prone to become anoxic due to water-saturated soil and the competition for $O_2$ with soil microorganisms. Lack of $O_2$ limits or abolishes respiration, the main source of energy in roots, and, as a consequence, impairs uptake of nutrients and water with severe

impact on growth and survival. Wetland plants have developed a variety of traits to alleviate the stresses caused by submergence. Rice (*Oryza sativa* L.) is a semi-aquatic plant with a strong tolerance to flooding. A number of adaptive traits in rice help maintain a functional root system during flooding (Pedersen *et al.*, 2020). One of these is the replacement of the primary root system by adventitious roots (ARs) that develop at the stem nodes. ARs grow into the upper soil layers or develop as floating roots when large portions of the stem are submerged (Zhang *et al.*, 2017; Lin and Sauter,

2018). In rice, the formation of AR primordia at the stem nodes is genetically determined, allowing plants to rapidly form a secondary root system from existing AR primordia (Lorbiecke and Sauter, 1999). Triggering of AR emergence is controlled by ethylene (Sauter, 2013) that accumulates in submerged plant parts due to the slow gas diffusion in water (Armstrong and Drew, 2002).

Previous studies on *Meionectes brownii* and *Alternanthera philoxeroides* suggested that floating ARs have multiple sources of $O_2$ (Rich *et al.*, 2013; Ayi *et al.*, 2016). $O_2$ can derive from the atmosphere, from the shoot via underwater photosynthesis, and/or from the floodwater. Floodwater often contains more $O_2$ than flooded soil due to a better aeration and underwater photosynthesis (Setter *et al.*, 1987). Submerged leaves continue to photosynthesize when light and $CO_2$ are available, which leads to production of $O_2$ as a by-product. Uptake of $O_2$ by ARs from the floodwater was shown for *A. philoxeroides* (Ayi *et al.*, 2016), but the mechanistic features that ensure $O_2$ supply of the growing root tip have not been studied in detail. In rice, $O_2$, from aerial or underwater photosynthesis, is released in either air or water, or accumulates in the aerenchyma or stem cavity. In rice, as in other aquatic or semi-aquatic plants, aerenchyma is formed in leaves, stems, and roots in adaptation and acclimation to their habitat. In addition, the cavity of cereal stems is an internal gas space and may facilitate diffusion of $O_2$ to ARs (Colmer, 2003; Mori *et al.*, 2019). Aerenchyma not only facilitates fast $O_2$ diffusion, it also decreases the number of $O_2$-consuming cells (Yamauchi *et al.*, 2013). While aerenchyma is constitutively formed in rice, this is not the case in maize (*Zea mays*) or wheat (*Triticum aestivum*) (Colmer and Voesenek, 2009). Studies on accessions of the wild relative of maize, teosinte (*Zea nicaraguensis*), indicated that constitutive aerenchyma determines tolerance to flooding (Mano and Omori, 2013). During flooding, aerenchyma formation is further enhanced in rice and induced in non-wetland species such as maize and barley (*Hordeum vulgare*), suggesting that aerenchyma formation is a universal flooding adaptation. Aerenchyma is fully developed in the mature root zone, whereas the root tip, where cell division and cell elongation take place, does not possess aerenchyma (Yamauchi *et al.*, 2017, 2019), raising the question of how the root tip with its high energy demand is supplied with $O_2$ (Yamauchi *et al.*, 2018).

In deoxygenated, stagnant nutrient solution (an experimental condition mimicking waterlogging), the formation of a barrier to radial $O_2$ loss (ROL) was reported for roots of rice, wheat amphiploids, and sea barleygrass (*Hordeum marinum*) (Colmer, 2003; Garthwaite *et al.*, 2006; Malik *et al.*, 2011). The barrier to ROL is formed at the walls of hypodermal/ exodermal cells (Armstrong *et al.*, 2000; Garthwaite *et al.*, 2008) and greatly restricts $O_2$ diffusion from the root to the anoxic soil (Colmer *et al.*, 1998; Soukup *et al.*, 2007). Restricted gas

diffusion is probably caused by suberin and/or lignin depositions (Kulichikhin *et al.*, 2014). Both aerenchyma and barrier formation were shown to improve $O_2$ supply to roots and to enhance overall root activity (Watanabe *et al.*, 2017; Pedersen *et al.*, 2020).

In this study, we analyzed the sources of $O_2$ supply to floating ARs to understand the ability of these roots to undergo rapid growth and survival as a response to submergence. We tested the hypothesis that floating roots of rice form abundant aerenchyma in combination with a barrier to ROL in order to sustain stem-derived diffusion of $O_2$ to the growing root tip. We assessed the contribution of the hollow stem versus floodwater as sources of $O_2$ to ARs and we visualized the tissue distribution of $O_2$ along the AR using a microsensor, and related these concentration gradients to the presence of aerenchyma and a barrier to ROL. Our study reveals that the root anatomical traits are well suited to specifically improve the $O_2$ status at the root tip. Our findings provide insight into the mechanisms that support root growth through improved $O_2$ supply to the root tip during flooding, an insight that might be applicable in the effort of producing climate-smart crops for a changing environment.

## Materials and methods

### *Plant material and submergence*

Seeds of the near-isogenic line 12 (NIL12 cv Taichung 65) were received from Motoyuki Ashikari (Nagoya University, Nagoya, Japan). The deepwater quantitative trait locus 12 (QTL-12) of the deepwater rice variety C9285 was introgressed into the lowland rice cultivar Taichung 65 to generate the NIL12 line (Hattori *et al.*, 2009). QTL-12 promotes rapid stem elongation when plants are partially submerged and the formation of floating ARs. Rice plants were grown in a 16 h, 360 μmol $m^{-2}$ $s^{-1}$ light, 27 °C/8 h dark, 19 °C cycle with a 30 min gradual light transition in the morning at 70% relative humidity. Plants were partially submerged in a 600 liter tank (Lorbiecke and Sauter, 1999; Sasidharan *et al.*, 2017) for 10–14 d. Water $O_2$ was measured with a microoptode (OP-MR, Unisense A/S) at a depth of 50 cm where plant material was collected. Measurements were taken at the onset and after 10 h of light.

### *$O_2$ measurement in floating adventitious roots*

An internode including the third youngest node (node 3) was collected with a cut 4 cm below node 3 and a cut 8 cm above it (Supplementary Fig. S1) (Lin *et al.*, 2020). All ARs except for one thick root of 8–10 cm (Figs 1, 2) were pruned at node 3 with a blade. The upper end of the internode was connected to a gas cylinder with a tube via a metal T-piece (Supplementary Fig. S1A). The stem section with the remaining AR was mounted with rubber bands on a wire sheet (Supplementary Fig. S1A, B) and the wire sheet was fixed on a beaker in an aquatic tank (25 cm length×15 cm width×10 cm height) that was filled with tap water to completely cover the root. An $O_2$ sensor in the tank monitored the water $O_2$ concentration. A microsensor with a 25 μm tip diameter (OX25, Unisense A/S) was fitted on a motorized stage (1D Motorized MicroProfiling System, Unisense A/S), connected to a picoampere meter (Field Multimeter, Unisense A/S, Denmark) and the sensor signals
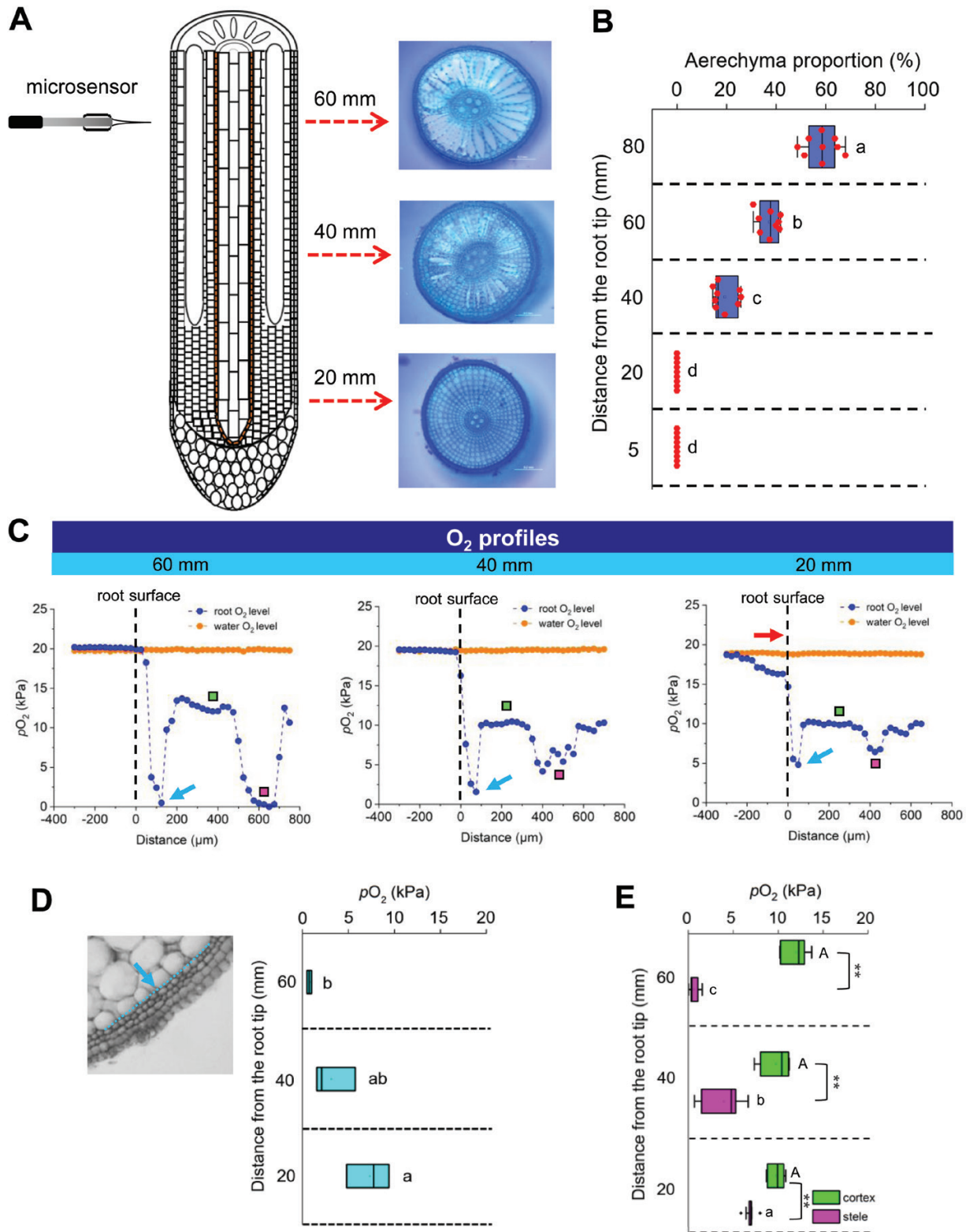
**Fig. 1.** Aerenchyma formation, radial $O_2$ profiles, and tissue $O_2$ status of aquatic adventitious roots of rice. (A) Cross-sections stained with toluidine blue; arrows indicate positions at which $O_2$ profiles were taken. (B) Percentage of aerenchyma formed at the positions indicated. Numbers are means (±SE) from three independent experiments with three different roots for each replicate ($n=9$, different letters indicate significant differences; $P<0.05$, Tukey test). (C) Radial $O_2$ profiles at the three distances behind the root tip indicated in (A). The $O_2$ microsensor was positioned 300 μm from the root surface and moved at steps of 25 μm until the tip of the sensor had passed the stele. The red arrow indicates the direction of gas diffusion; blue arrows point to the border between outer cell layers and the cortex. Green and magenta squares indicate the cortex and stele, respectively. (D) The lowest $O_2$ level between outer cells, made up of four cell layers as shown in the cross-section, and cortex. The blue arrow points to the border between outer cell layers and the cortex. Results are means (±SE, $P<0.05$; Tukey test) from three floating adventitious roots analyzed at each position indicated. (E) Mean $O_2$ levels in the cortex or the stele from three

were collected with a frequency of 1 Hz using data acquisition software (Sensortrace Suite version 2.3.100, Unisense A/S). At the onset of a measurement, the sensor tip was placed at a distance of 300 μm from the root surface. The sensor was moved stepwise toward and into the root at 25 μm per step, and $O_2$ was measured at each step. The measurement was stopped at ~750 μm inside the root when the microsensor had passed the central cylinder of the root. Where indicated, the same root was measured at 20, 40, and 60 mm from the root tip.

During measurements, the water in the tank was bubbled with air to increase gas diffusion between the root and the water. To analyze the gas exchange between the root tip and the water, the stem was supplied with 100% $O_2$ or 100% $N_2$ starting 40 min prior to the measurement and $O_2$ was monitored with an $O_2$ sensor placed in the T-piece (Supplementary Fig. S1A). A microsensor was placed 20 mm from the root tip that traced $O_2$ starting at 250 μm from the root surface to ~800 μm inside the root, past the central cylinder, in 25 μm steps as described.

To investigate whether $O_2$ supplied through the internode altered $O_2$ in the root, a microsensor was inserted in the cortex of the mature root zone 6.4 cm from the root tip at a depth of 150 μm. Water was bubbled with $N_2$ until the $O_2$ in the water reached 7.5 kPa (~100 mol l$^{-1}$). Subsequently, the internode was supplied with 100% $O_2$ and measurement continued until the $O_2$ in the root was saturated. Then, the internode was supplied with 100% $N_2$ until the $O_2$ in the root was stable. Finally, the internode was supplied with air and measurement continued until the root $O_2$ was stable.

To analyze gas diffusion through nodes, a stem section was cut from the first internode to 4 cm below node 3. Gas was supplied through the first internode so that the gas had to pass two nodes before it reached the root at node 3 (Fig. 5A). After each measurement, stems were cut longitudinally to ensure that no water had leaked inside the stem (Supplementary Fig. S1B). A cross-section of the root was cut at the site of measurement to visualize the microsensor track (Supplementary Fig. S1C).

*Aerenchyma, calculations of $O_2$ fluxes, and permeability test*

Roots were embedded in 5% (w/v) agar to obtain 100 μm cross-sections with a vibratome (HYRAX V50, Zeiss). Sections were stained with 1% (w/v) toluidine blue, washed three times with distilled water, and visualized (Nikon H600L, Japan). Aerenchyma was calculated by dividing the aerenchyma area by the total cortex area.

$O_2$ fluxes were calculated according to Henriksen *et al.* (1992). $O_2$ fluxes between roots and floodwater were calculated based upon the concentration gradients in the diffusive boundary layer enveloping the roots. Positive fluxes indicate ROL to the floodwater and negative fluxes indicate radial $O_2$ consumption (ROC) from the floodwater. The calculations used the equation from Henriksen *et al.* (1992):

$$J = \frac{D_i}{r_0} \frac{c_{100} - c_0}{\ln(r_{100}/r_0)}$$

where $J$ (mol m$^{-2}$ s$^{-1}$) is the flux, $D_i$ is the diffusion coefficient at 25 °C of $O_2$ (2.2×10$^{-9}$ m$^2$ s$^{-1}$; Ferrell and Himmelblau, 1967), $r_0$ (m) is the radius of the root, $r_{100}$ (m) is the radius of the root+100 μm (=0.0001 m), $c_0$ is the dissolved $O_2$ (mol m$^{-3}$) at the root surface, and $c_{100}$ is the dissolved $O_2$ concentration (mol m$^{-3}$) 100 μm away from the root surface. The values of dissolved gas concentrations at the two positions within the diffusive boundary layer were derived from the linear regression of the $O_2$ data from profiling conducted using microsensors.

Permeability of epidermal cells was tested with 0.1% (w/v) of the apoplastic tracer periodic acid. After 1 h, a reducing solution (1 g of KI and 1 g of $Na_2S_2O_3$ in 50 ml of distilled water acidified with 5 M HCl) was applied overnight to remove excess stain. Schiff's reagent revealed periodic acid in purple.

*Cellulose, suberin, lignin, and sclerenchyma staining*

Sclerenchyma were visualized with toluidine blue. Cross-sections of nodes were stained for cellulose with 1.5% (w/v) astrablue for 5 min and washed twice with distilled water. Subsequently, the sections were stained with 0.5% (w/v) safranin for 5 min and washed twice with 70% ethanol to visualize lignin in pink. Suberin was visualized in cross-sections after incubation in 0.1% (w/v) fluorol yellow 088 in the dark for 1 h and two washing steps in 75% glycerol under UV light (BX41, OLYMPUS). Lignin was stained in cross-sections and roots with 1% (w/v) phloroglucinol for 1 h, followed by dipping in 6 M HCl for 10 min.

*Statistical analysis*

Statistical analyses were performed using Minitab. Comparison of means was performed for statistical significance with an ANOVA Tukey test or two-sample *t*-test. Constant variance and normal distribution of data were verified before statistical analysis. The *P*-value was set to $P<0.05$.

## Results

*The mature root zone relies on $O_2$ supply from the stem whereas the root tip can also obtain $O_2$ from the floodwater*

Our model plant NIL12 is a near-isogenic line of rice with a deepwater rice trait introduced in paddy rice promoting stem elongation in response to flooding (Hattori *et al.*, 2009). NIL12 also grows substantially more ARs compared with the paddy rice (Supplementary Fig. S2A) and consequently NIL12 serves as an excellent model to study tissue aeration of floating ARs as an adaptation to deep water. For a better comparison of internal aeration and anatomical features, all experiments were performed on 8–10 cm long and thick ARs (Supplementary Fig. S2B) as a root model.

To assess the $O_2$ diffusion capacity of the root, we determined aerenchyma formation from cross-sections at 20, 40, 60, and 80 mm behind the tip (Fig. 1A, B). At 20 mm, the cortex was intact, whereas at 40 mm, aerenchyma had formed in the middle cortex cell layers occupying 19% of the cross-sectional cortex area (Fig. 1B). At 60 mm, aerenchyma extended to the outer cortex cells, reaching 37%, and at 80 mm, aerenchyma reached 58%, in agreement with a similar study on aerenchyma development in rice roots (Yamauchi *et al.*, 2019).

Root tissue $O_2$ status was obtained with high spatial resolution at positions 20, 40, and 60 mm behind the root tip of floating

floating adventitious roots analyzed at each position. Upper case letters indicate the statistical difference between the cortex at three positions ($P<0.05$, Tukey test). Lower case letters indicate the statistical difference between the stele at three positions ($P<0.05$, Tukey test). Asterisks indicate the statistical difference between the cortex and the stele at each position ($P<0.01$, ANOVA with Student *t*-test). Different letters indicate significant differences; $P<0.05$, Tukey test.
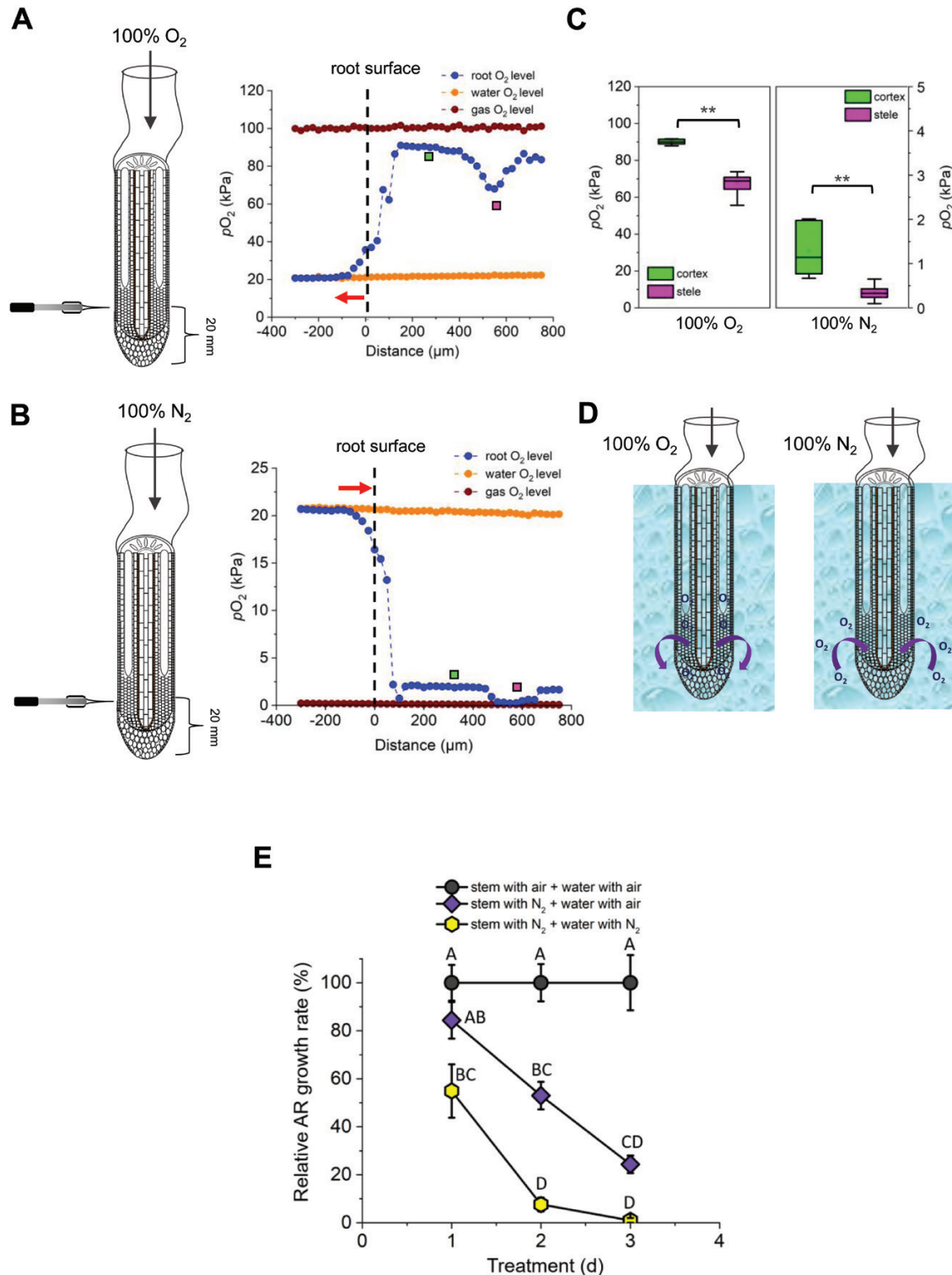
**Fig. 2.** The growing tip of aquatic adventitious roots receives $O_2$ from the stem and the water. (A) The cut end of the internode was supplied with 100% $O_2$ and the radial $O_2$ profile was determined at 20 mm behind the root tip. The red arrow indicates the direction of $O_2$ diffusion. Green and magenta squares indicate the cortex and stele, respectively. (B) The cut end of the internode was supplied with 100% $N_2$ and the radial $O_2$ profile determined at 20 mm behind the root tip. The red arrow indicates the direction of $O_2$ diffusion. Green and magenta squares indicate the cortex and stele, respectively. (C) Mean $O_2$ levels in the cortex or the stele resulting from the manipulated gas supply to the cut end of the stem as extracted from (A) or (B). Asterisks indicate statistically significant differences (means± SE, $n=9$, $P<0.01$, ANOVA with Student $t$-test). (D) Scheme indicating that the root tip can obtain $O_2$ from the internode and from the surrounding water depending on predominant $O_2$ gradients. (E) Growth of ARs supplied with $O_2$ from the stem and the water, from the water only, or with no $O_2$ (for setup and absolute growth data, see Supplementary Figs S5 and S6). Growth rates were normalized to the values obtained with $O_2$ supply to the stem and water at each time point for better comparison. Different letters indicate statistical differences between treatments over time ($n=18$–23, ANOVA with Tukey test, $P<0.05$).

ARs using $O_2$ microsensors mounted on a micromanipulator (Supplementary Fig. S3). $O_2$ concentrations were recorded starting 300 μm away from the root surface in the floodwater, taking measurements at steps of 25 μm until the tip of the sensor had passed the central cylinder (Supplementary Figs S1C, S3). In the submergence tanks used to trigger formation of floating ARs, the $O_2$ partial pressure was on average 22.1 kPa in the light period (Supplementary Fig. S4). To mimic floodwaters, we used air-bubbled tap water to maintain $O_2$ at 20.6 kPa in the experimental tank and we continuously recorded floodwater $O_2$ with a separate $O_2$ sensor (Fig. 1C; Supplementary Fig. S3). At 60 mm, the $O_2$ partial pressure at the root surface was similar to that of the floodwater. In contrast, the $O_2$ partial pressure at the root surface declined at 40 mm and even more so at 20 mm, suggesting that water $O_2$ was consumed by the root (Fig. 1C). At 20 mm, the $O_2$ concentration in the water declined close to the root surface, resulting in a ROL of −737 nmol $m^{-2}$ $s^{-1}$ (Table 1), confirming that $O_2$ diffused from the floodwater into the root tip. In the outer cell layers, within the first 100 μm, the $O_2$ partial pressure decreased to 0.7 kPa at 60 mm, to 3.1 kPa at 40 mm, and to 7.3 kPa at 20 mm (Fig. 1C, D), confirming that $O_2$ can diffuse through these cell layers with much lower resistance at the tip compared with the base. In the cortex, the $O_2$ partial pressure was 12.0 kPa at 60 mm, 9.7 kPa at 40 mm, and 9.8 kPa at 20 mm (Fig. 1C). Even though the differences were not statistically significant (Fig. 1E), they are in accordance with the observation that aerenchyma development is more pronounced in the mature part, facilitating $O_2$ diffusion from the shoot. The $O_2$ partial pressure in the stele approached 0 kPa at 60 mm, was 3.9 kPa at 40 mm, and 6.8 kPa at 20 mm (Fig. 1C, E), revealing a better $O_2$ supply at the root tip compared with the base.

Taken together, our results showed that the epidermal cells and the stele are better supplied with $O_2$ at the root tip than in the mature root zone. The improved $O_2$ supply of the root tip in part results from $O_2$ diffusing into the tissue from the surrounding floodwater. To obtain a more comprehensive understanding of the mechanisms behind $O_2$ supply to the root tip, we next studied the gas exchange between ARs and internodes or floodwater in more detail.

**Table 1.** Oxygen flux between water and the root tip

| Stem treatment | Radial oxygen loss (nmol $m^{-2}$ $s^{-1}$) |
| --- | --- |
| 0% $O_2$ | −1103.7±96.6 a |
| 21% $O_2$ | −737±85.2 b |
| 100% $O_2$ | 4827±615.6 c |

$O_2$ flux at 20 mm behind the root tip was measured with $O_2$ in air equilibrium in the floodwater and supplying the cut end of the internode with 100% $N_2$, 21% $O_2$+79% $N_2$, or 100% $O_2$. Positive values indicate $O_2$ diffusion from the root to the water (radial oxygen loss) and negative values indicate $O_2$ diffusion from the water into the root. Different letters indicate significant differences between treatments (means ±SE, *P*<0.05, Mann–Whitney test).

### $O_2$ exchange between the root tip and floodwater is determined by tissue $O_2$ status

The fine details of $O_2$ exchange between the root tip and floodwater were visualized by supplying the hollow stem with pure $O_2$ (Fig. 2A; Supplementary Fig. S3A). After the cut end of the stem had been exposed to 100% $O_2$ for 40 min, tissue $O_2$ status at the root tip was greatly elevated. However, the radial $O_2$ profile showed a very similar pattern to the one observed previously (Fig. 1); $O_2$ in the epidermal cell layers and in the stele was much lower than in the cortex (Fig. 2A). The $O_2$ concentration in the water close to the root surface increased over the ambient water $O_2$ concentration (Fig. 2A), clearly showing that $O_2$ diffused from the root into the floodwater, as further confirmed by the calculated ROL flux (4827 nmol $O_2$ $m^{-2}$ $s^{-1}$, Table 1).

We next exposed the cut end of the stem to pure $N_2$ to reduce $O_2$ concentration in the pith cavity in the root (Fig. 2B). This treatment resulted in a substantial reduction in $O_2$ in the outer cell layers of the root and generated a severely hypoxic core within the stele while the cortex maintained 1 kPa $O_2$ (Fig. 2C). With this treatment, the $O_2$ concentration at the root surface decreased compared with ambient water $O_2$, indicating that $O_2$ diffused from the floodwater and into the root tip (Fig. 2C) as confirmed by the calculated ROL of −1104 nmol $m^{-2}$ $s^{-1}$, which was significantly higher than the flux that occurred with supply of 21% $O_2$ to the cut end of the stem (Table 1).

Under natural conditions, the $O_2$ concentration in the floodwater depends on various environmental conditions (Pedersen *et al.*, 2017), thereby exposing floating roots to varying $O_2$ levels that can range from higher than normoxia to hypoxia (Rich *et al.*, 2013; Loreti *et al.*, 2016). Tissue $O_2$ gradients within the ARs were similar but at vastly different amplitudes when the stem was supplied with either 100% $O_2$ or 100% $N_2$.

To test if $O_2$ uptake through the root tip was sufficient to support root growth, we compared root growth rates under conditions where $O_2$ was supplied (i) from the stem and the floodwater; (ii) exclusively from the floodwater; or (iii) with no $O_2$ at all (Fig. 2E; Supplementary Figs S5, S6). The results revealed an intermediary growth rate in ARs supplied with $O_2$ from the floodwater to the root tip with higher growth rates when the stem also provided $O_2$ and lower growth rates in roots not receiving $O_2$. In conclusion, the root tip was able to benefit from $O_2$ in the floodwater when supply from the internode was limited, revealing a mechanism by which growth can be sustained by $O_2$ supply to the growing root tip either from the shoot or from the floodwater depending on the environmental conditions (Fig. 2D).

### Suberin and lignin depositions increase in the outer cell layers during root maturation and are likely to form a barrier for radial $O_2$ loss

To compare the permeability at the root tip with that of mature root zones, the apoplastic tracer periodic acid was employed. At 60 mm and 40 mm from the tip of floating ARs
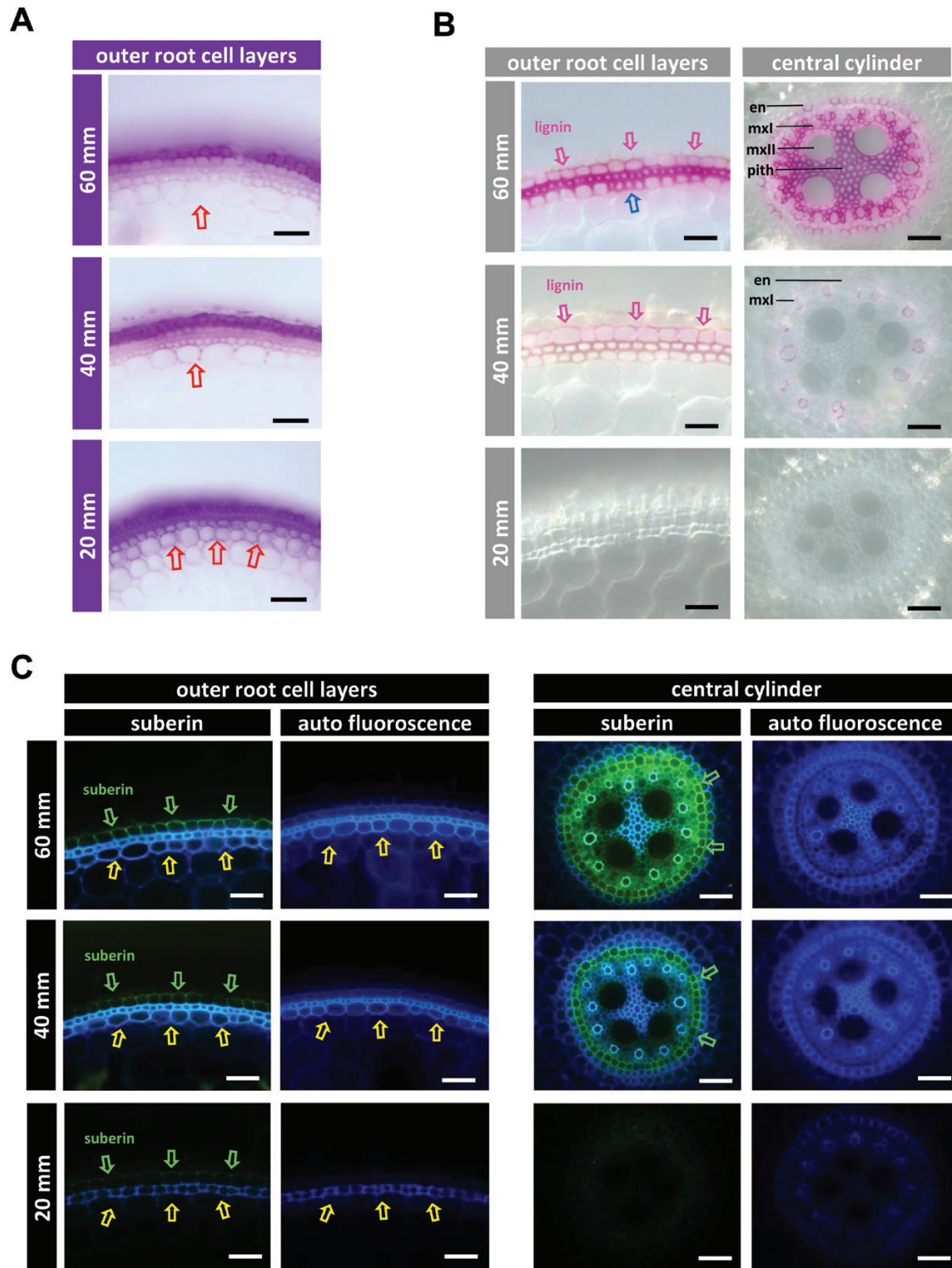
**Fig. 3.** The outer cell layers of aquatic adventitious roots of rice have lower suberin and lignin levels and are more permeable at the root tip than in the mature root zone. (A) The diffusion barrier increases from root tip to base. Cross-sections reveal diffusion of periodic acid in the apoplast at the distance behind the root tip indicated. Red arrows point to the outermost layer of cortex cells. The blue arrow points to patches of cells with thickened cell walls. Scale bar=20 μm. (B) Lignification of the outer cell layers and the central cylinder is visible at 40 mm and further enhanced at 60 mm, but is not observed at all at 20 mm behind the root tip. Lignin is stained pink and indicated by pink arrows. Scale bar=20 μm. (C) The formation of suberin increases from root tip to base in the outer cell layers and the stele. Suberin lamellae are visualized in yellow-green color indicated by green arrows. Yellow arrows point to cell wall autofluorescence. Scale bar=20 μm.

of partially submerged plants, the tracer permeated only the outermost cell layer, whereas at 20 mm all four epidermal cell layers were permeable, indicating that the mature root zones but not the root tip possess an apoplastic barrier that blocks radial diffusion (Fig. 3A).

Since the root tip but not the mature root zones were permeable to $O_2$ and periodic acid, we next asked whether a barrier for ROL was formed at the basal part of the root that restricted $O_2$ diffusion between root and floodwater. Suberin and lignin are two main components of barriers to ROL that were described previously (Shiono *et al.*, 2014) and we therefore analyzed suberization and lignification of the root (Figs 3B, C). Cross-sections were prepared at 20, 40, and 60 mm, and stained with phloroglucinol for lignin (Fig. 3B). No lignin was detected at 20 mm behind the root tip. At 40 mm, weak staining appeared at the outer root cell layers and in the central cylinder. At 60 mm, strong staining was detected in the outer cells, most predominantly in the third outermost cell layer that had sclerenchymatous walls (Supplementary Fig. S7). In the fourth cell layer, cells occasionally developed thick, lignified walls (Fig. 3B). In addition to the root surface, lignin was also detected in cell walls of the endodermis and central cylinder at 60 mm. The heavy lignification of the stele may explain the very low $O_2$ concentration measured inside the stele (Fig. 1C).

Fluorol yellow 088 was used to visualize suberin lamellae as a yellow–green stain (Fig. 3C). At 20 mm, suberin was detected in walls of the second outermost cell layer, and suberin staining appeared stronger at 40 mm and 60 mm. Suberin-derived fluorescence was also seen in the central cylinder (Fig. 3C) where it was weak at 20 mm, increased at 40 mm, and further increased at 60 mm, and was mainly present in the endodermis. Analysis of AR primordia and emerged ARs showed that no suberin or lignin was deposited at these early developmental stages (Supplementary Fig. S8) in accordance with the finding that root tips are highly permeable.

In conclusion, our results revealed increasing deposition of suberin and lignin in the outer cell layers of the root and in the stele from tip to base. The increasing degree of cell wall modification inversely correlates with the root permeability to $O_2$ in the epidermal cell layers and in the stele.

### The $O_2$ status in the mature root zone is determined by the $O_2$ supply from the internode

The rice internode is a hollow structure with a central cavity enabling fast diffusion of $O_2$ in gas phase (Stünzi and Kende, 1989) (Fig. 5B). We tested the importance of the internode for $O_2$ supply to ARs by measuring $O_2$ profiles of ARs at 65 mm from the root tip in the mature root zone that had well-developed aerenchyma (Fig. 4A). An $O_2$ microsensor was placed in the cortex 150 μm from the root surface (Fig. 4B) and the floodwater was bubbled with 100% $N_2$. This treatment decreased the $O_2$ partial pressure in the water from 20.4 kPa to 7.5 kPa whereas the $O_2$ level inside the root did not
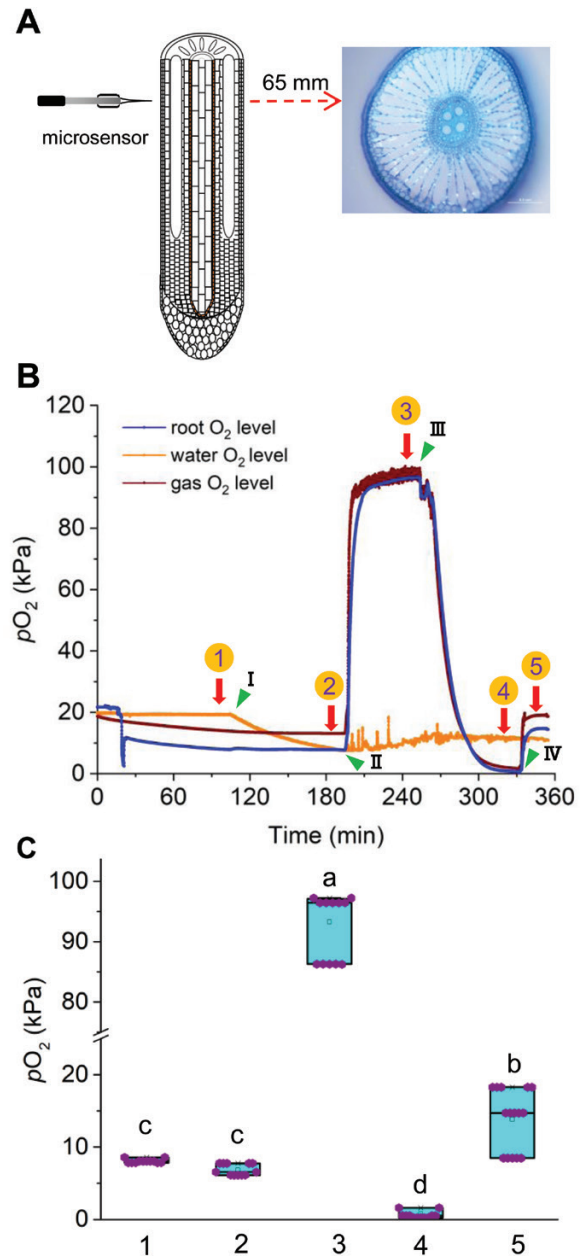


**Fig. 4.** The mature part of floating adventitious roots of rice is mainly supplied with $O_2$ from the internode. (A) Scheme showing the experimental setup to measure $O_2$ supply from the internode to a root submerged in water, indicating the position of the microsensor that was inserted into the cortex at a depth of 125 μm. Treatments were continued until the $O_2$ level in the root had reached a new quasi-steady-state. The cross-section at the position analyzed reveals a highly developed aerenchyma. (B) The root was exposed to an alternating $O_2$ regime that is indicated by Roman numerals: I, water flushed with 100% $N_2$; II, internode supplied with 100% $O_2$; III, internode supplied with 100% $N_2$; IV, internode supplied with air. The quasi-steady-state $O_2$ levels are indicated by Arabic numerals. 1, $O_2$ in the root with the internode supplied with air; 2, $O_2$ in the root when the water is flushed with $N_2$; 3, $O_2$ in the root when the internode is supplied with 100% $O_2$; 4, $O_2$ in the root when the internode is supplied with 100% $N_2$; 5, $O_2$ in the root when the internode is supplied with air. (C) $O_2$ levels following the treatments described in (B). Different letters indicate significant differences ($P<0.05$, one-way ANOVA with Tukey test).
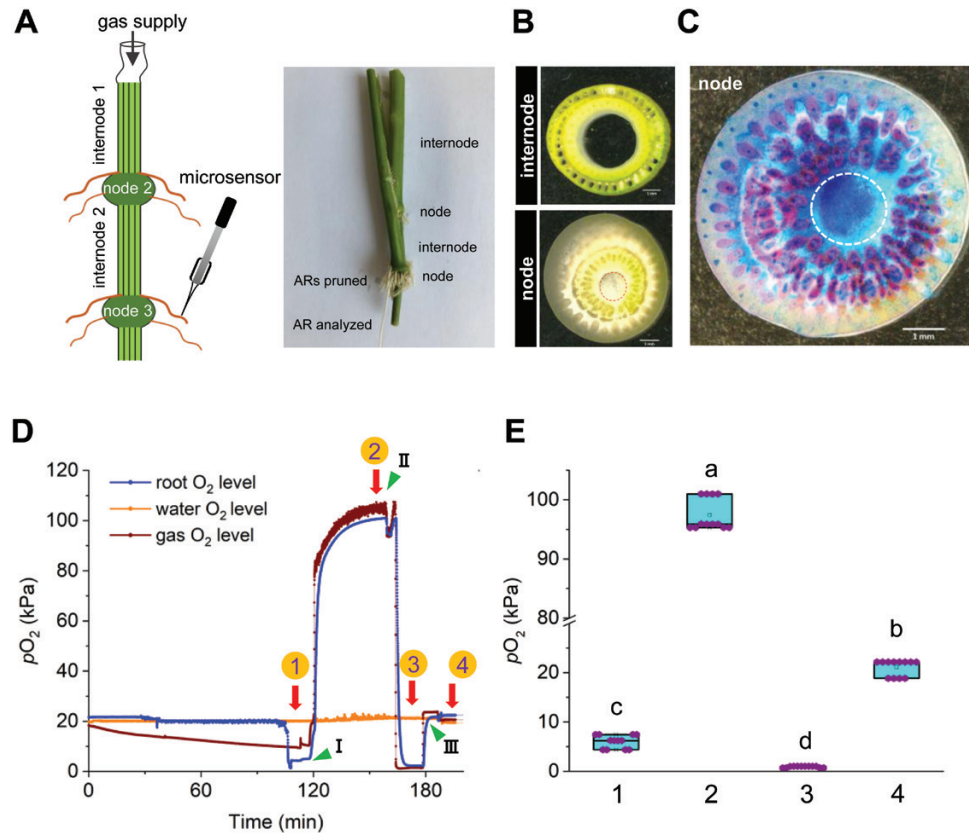
**Fig. 5.** Nodes do not restrict $O_2$ diffusion from internode to internode. (A) Scheme showing the experimental setup. A stem with two nodes was used and gas was provided to the cut end of the upper internode (internode 1), and the microsensor was inserted 125 μm into the cortex at 65 mm behind the tip of a root emerging from the lower node (node 3). (B) Cross-sections of an internode with leaf sheath and nodes. The dashed line in the nodal cross-sections delimits the spongy center. (C) Astrablue staining of cellulose (blue) and safranin staining of lignin (pink) revealed little cell wall differentiation in the spongy center of the node delimited by a dashed line. (D) $O_2$ level in the cortex under the treatments indicated by Roman numerals: I, internode supplied with 100% $O_2$; II, internode supplied with 100% $N_2$; III, internode supplied with air. The $O_2$ measurements were performed when $O_2$ was at a quasi-steady-state: 1, $O_2$ in the root without treatment; 2, $O_2$ in the root when the upper internode was supplied with 100% $O_2$; 3, $O_2$ in the root when the upper internode was supplied with 100% $N_2$; 4, $O_2$ in the root when the upper internode was supplied with air. (E) Average (means ±SE, $n=3$, $P<0.05$; one-way ANOVA with Tukey test) $O_2$ levels in the root after treatments indicated in (D) were determined from three independent experiments. Statistically significant differences are indicated by different letters.

change significantly (Fig. 4C). The fact that tissue $O_2$ does not respond to declining external $O_2$ is consistent with our observation that a barrier to ROL is formed at the root base (Fig. 3) that effectively prevents $O_2$ from diffusing from the root into the water, or vice versa. Subsequently, the internode was supplied with 100% $O_2$ which resulted in a rapid increase in root $O_2$ to almost 100 kPa, indicating that $O_2$ diffused freely from the internode to the root. When the $O_2$ level in the root reached an equilibrium, the internode was supplied with 100% $N_2$ which caused an immediate decline in root $O_2$ level that reached close to 0 kPa after 1 h. In the final step of the gas manipulation, the internode was supplied with ambient air which brought the root $O_2$ level back to 15 kPa within 15 min. Taken together, the $O_2$ concentration in the basal part of the root closely followed the $O_2$ level in the internode which is the major source of $O_2$ for the mature root zone.

In flooded deepwater rice, a vertical $O_2$ gradient develops, with higher $O_2$ levels in the upper internode compared

with lower internodes (Stünzi and Kende, 1989), raising the question of whether gas diffusion between internodes is limited by the nodes that separate them (Fig. 5A). To explore whether longitudinal gas movement in the rice stem is restricted by nodes that consist of a spongy tissue (Fig. 5B, C), we supplied gas to internode 1 and analyzed $O_2$ in a root that grew from node 3 (Fig. 5A). When the internode was supplied with 100% $O_2$, the root $O_2$ rapidly increased to a similar level in the root cortex (Fig. 5D, E). Supply of $N_2$ to the internode caused a rapid drop in root $O_2$ to near zero, while supply with air led to a recovery of the root $O_2$ to ~19 kPa (Fig. 5D, E). In conclusion, the results show that nodes have a high gas permeability and are not restricting $O_2$ supply from the shoot to the ARs. Our observations further support the conclusion that the internode is the main source of $O_2$ for the mature zone of the floating ARs. The sources and diffusion paths of $O_2$ in aquatic rice ARs are conceptualized in Fig. 6.
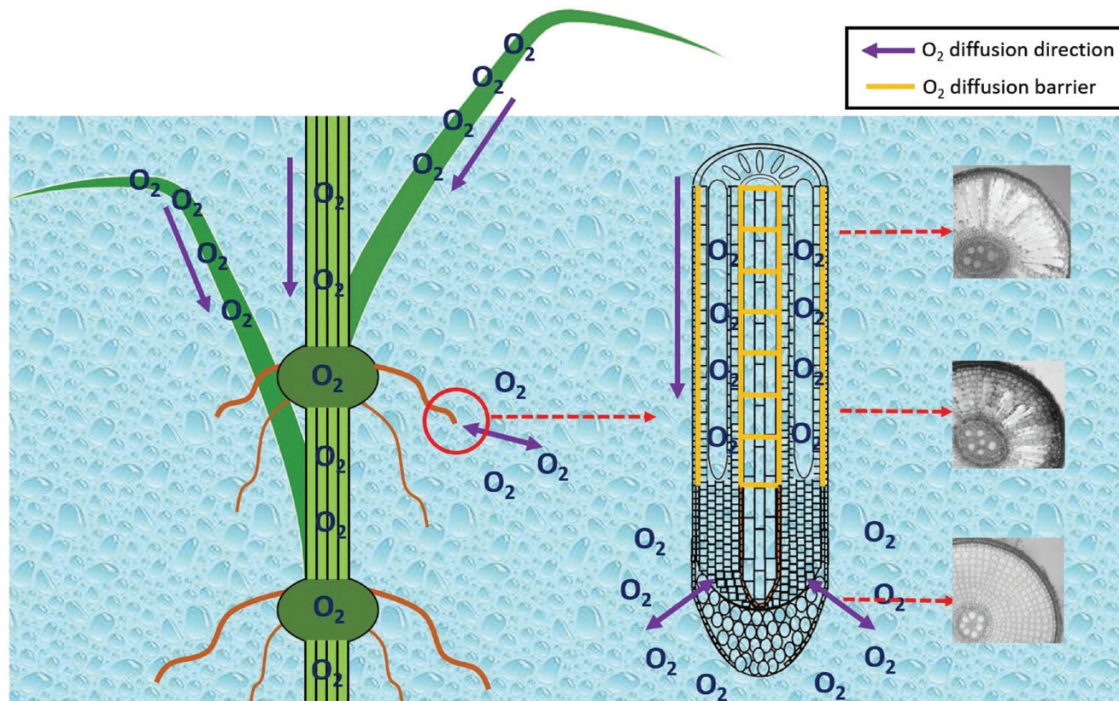
**Fig. 6.** Conceptual model of $O_2$ supply to floating adventitious roots of rice. $O_2$ sources of the stem of deepwater rice have recently been identified by Mori *et al.* (2019) and were therefore not included in the present study. In brief, these authors showed that $O_2$ can diffuse from the floodwater and into the leaves and further into the stem; the diffusion is enhanced in the presence of leaf gas films. Moreover, snorkelling (the shoot emerging partially into the air) further enhanced $O_2$ supply to the submerged part of the stem. The mature zone of the floating AR relies exclusively on $O_2$ diffusing from the stem. Root tips receive $O_2$ from the stem and rely on $O_2$ dissolved in the floodwater that diffuses into the tissue in the absence of a diffusion barrier.

## Discussion

Rice responds to submergence by growing a large number of ARs from submerged stem nodes. The sources of $O_2$ for these floating ARs were not previously known. The present study revealed that $O_2$ from the stem primarily sustains the mature zones of the roots, whereas the immature, growing root tip obtains $O_2$ from the stem and the floodwater. Below, we discuss these findings in further detail with emphasis on the mechanisms behind $O_2$ supply of the growing root tip.

### *The tip of floating adventitious roots acquire $O_2$ from the water*

Many wetland plants develop floating ARs, including the halophyte *Tecticornia pergranulata* (Pedersen *et al.*, 2006) and the semi-aquatic wetland plant *Meionectes brownii* (Rich *et al.*, 2013). In both species, the root $O_2$ status closely followed that of the surrounding water during the night-time whereas daytime root $O_2$ was of photosynthetic origin from the shoot (*T. pergranulata*) or from green photosynthetic roots (*M. brownii*), with no indication that aquatic roots had formed a barrier to ROL. In contrast, the mature zone of aquatic rice ARs developed a barrier to ROL in long-term flooding. The walls of the four cell layers of the hypodermis/

exodermis gradually deposit suberin and lignin during AR differentiation. Suberin is suggested to reduce the gas permeability, whereas the gas permeability of lignin has not been tested (Watanabe *et al.*, 2013). In the central cylinder, suberin accumulated in endodermal cell walls and lignin accumulated in the endodermis and throughout the stele, indicating that floating roots develop two diffusion barriers while maturing, one at the root–water interface and one at the cortex–stele interface. Barrier formation was inversely related to the $O_2$ concentration in the central cylinder and led to a steep $O_2$ gradient between cortex and stele in the mature root. The root tip showed minor suberin and no lignin accumulation, and the $O_2$ level in the stele reached ~7 kPa, revealing that, despite the lack of aerenchyma, the root apex was better oxygenated than the mature root.

Local barrier formation has an impact on $O_2$ supply. The mature root zone receives $O_2$ exclusively from the shoot, whereas the tip receives $O_2$ from the shoot and the floodwater (Fig. 6). The internal and external diffusion barriers, the aerenchyma in the mature root zone and porosity at the root tip, channel $O_2$ to the root tip (Armstrong, 1971; Colmer, 2003). When supply of ARs with $O_2$ from the stem is limited due to low photosynthetic activity in muddy waters or at night, $O_2$ influx from the water may occur at the root tip which then contributes to improved aeration of the root apex over the mature root zone

(Ayi *et al.*, 2016). $O_2$ uptake at the root tip is in fact sufficient to support root growth and possibly other root functions.

While dryland crops, such as wheat, maize, and barley, do not form aerenchyma unless they are flooded (Yamauchi *et al.*, 2013; Zhang *et al.*, 2015), aerenchyma constitutively forms in rice roots, which, to some extent, determines its flooding tolerance (Yamauchi *et al.*, 2017, 2019). However, even though soil roots develop aerenchyma, flooding induces the emergence of ARs from the stem nodes, suggesting that the investment made in generating floating ARs is worthwhile for the plant presumably because these support or replace the primary root system (Jackson and Drew, 1984; Colmer and Greenway, 2011; Zhang *et al.*, 2017). Unlike water-saturated soil, floodwater is generally oxygenated depending on temperature, water depth, $O_2$ consumption, and underwater photosynthesis (Setter *et al.*, 1987; Phan-Van *et al.*, 2008; Ayi *et al.*, 2016). In our experimental setup, water $O_2$ reached up to 20 kPa in the light, suggesting that $O_2$ uptake from the water can occur under common environmental conditions and contribute to the $O_2$ supply of the ARs which may be a decisive advantage over soil-borne roots.

### $O_2$ diffusion is not restricted at the stem nodes

Unlike the stem that develops aerenchyma, nodes contain vasculature and root primordia embedded in spongy tissue, but no aerenchyma (Fig. 5C) (Steffens *et al.*, 2011; Yamaji and Ma, 2014). Nonetheless, the $O_2$ of the internode equilibrates rapidly with the root even across nodes, indicating that $O_2$ diffusion is not limiting. The $O_2$ in the internode is dynamic and can vary depending on environmental conditions and adaptive plant features. It follows a diurnal pattern, with lower $O_2$ in the dark due to respiration and higher $O_2$ in the daytime as a result of photosynthesis (Stünzi and Kende, 1989; Mori *et al.*, 2019). Internodal $O_2$ is further determined by the water level (Mori *et al.*, 2019) and can differ between partial and complete submergence. Consequently, $O_2$ supply of aquatic roots by the stem varies depending on environmental conditions. Unlike the mature root, the root tip can partially compensate for limited $O_2$ supply from the stem by $O_2$ uptake from floodwater.

In conclusion, flooding induces growth of aquatic ARs that is supported by $O_2$ supplied to the apex from the shoot and from the floodwater. Funnelling of $O_2$ from the root base to the tip is facilitated by aerenchyma that favors longitudinal diffusion and by diffusion barriers that prevent radial loss of $O_2$ in the mature root zone. $O_2$ exchange between the water and the root occurs at the root tip, thereby providing an alternative source of $O_2$ to the growth region.

## Supplementary data

The following supplementary data are available at *JXB* online.
Fig. S1. Experimental setup used for the analysis of root $O_2$.

Fig. S2. NIL12 plants develop more ARs than T65 plants.
Fig. S3. Experimental setup used to investigate $O_2$ supply to aquatic ARs.
Fig. S4. Floodwater $O_2$ in the light.
Fig. S5. Effect of $O_2$ and $N_2$ supply from the stem and floodwater on root growth.
Fig. S6. Effect of $O_2$ supply from the stem and floodwater on root growth.
Fig. S7. Cell wall thickening in epidermal cells.
Fig. S8. Adventitious root primordia and early stage ARs are not suberized or lignified.

## Acknowledgements

## Author contributions

CL, OP, and MS designed the project and the experiments; CL, LLPO, and OP performed and analyzed the experiments, CL, OP. and MS wrote the manuscript.

## Data availability

The data supporting the findings of this study are available from the corresponding author, Margret Sauter, upon request.

## References

**Armstrong W.** 1971. Radial oxygen losses from intact rice roots as affected by distance from the apex, respiration and waterlogging. Physiologia Plantarum **25**, 192–197.

**Armstrong W, Cousins D, Armstrong J, Turner DW, Beckett PM.** 2000. Oxygen distribution in wetland plant roots and permeability barriers to gas-exchange with the rhizosphere: a microelectrode and modelling study with *Phragmites australis*. Annals of Botany **86**, 687–703.

**Armstrong W, Drew MC.** 2002. Root growth and metabolism under oxygen deficiency. In: Waisel Y, Eshel A, Kafkafi U, eds. Plant roots: the hidden half, 3rd edn. Marcel Dekker, 1139–1187.

**Ayi Q, Zeng B, Liu J, Li S, van Bodegom PM, Cornelissen JHC.** 2016. Oxygen absorption by adventitious roots promotes the survival of completely submerged terrestrial plants. Annals of Botany **118**, 675–683.

**Chen H, Liang Z, Liu Y, Jiang Q, Xie S.** 2018. Effects of drought and flood on crop production in China across 1949–2015: spatial heterogeneity analysis with Bayesian hierarchical modeling. Natural Hazards **92**, 525–541.

**Colmer TD.** 2003. Aerenchyma and an inducible barrier to radial oxygen loss facilitate root aeration in upland, paddy and deep-water rice (*Oryza sativa* L.). Annals of Botany **91**, 301–309.

**Colmer TD, Gibberd MR, Wiengweera A, Tinh TK.** 1998. The barrier to radial oxygen loss from roots of rice (*Oryza sativa* L.) is induced by growth in stagnant solution. Journal of Experimental Botany **9**, 1431–1436.

**Colmer TD, Greenway H.** 2011. Ion transport in seminal and adventitious roots of cereals during $O_2$ deficiency. Journal of Experimental Botany **62**, 39–57.

**Colmer TD, Pedersen O.** 2008. Underwater photosynthesis and respiration in leaves of submerged wetland plants: gas films improve $CO_2$ and $O_2$ exchange. New Phytologist **177**, 918–926.

**Colmer TD, Voesenek LACJ.** 2009. Flooding tolerance: suites of plant traits in variable environments. Functional Plant Biology **36**, 665–681.

**Ferrell RT, Himmelblau DM.** 1967. Diffusion coefficients of nitrogen and oxygen in water. Journal of Chemical and Engineering Data **12**, 111–115.

**Garthwaite AJ, Armstrong W, Colmer TD.** 2008. Assessment of $O_2$ diffusivity across the barrier to radial $O_2$ loss in adventitious roots of *Hordeum marinum*. New Phytologist **179**, 405–416.

**Garthwaite AJ, Steudle E, Colmer TD.** 2006. Water uptake by roots of *Hordeum marinum*: formation of a barrier to radial $O_2$ loss does not affect root hydraulic conductivity. Journal of Experimental Botany **57**, 655–664.

**Hattori Y, Nagai K, Furukawa S, et al.** 2009. The ethylene response factors *SNORKEL1* and *SNORKEL2* allow rice to adapt to deep water. Nature **460**, 1026–1030.

**Henriksen GH, Raman DR, Walker LP, Spanswick RM.** 1992. Measurement of net fluxes of ammonium and nitrate at the surface of barley roots using ion-selective microelectrodes: II. Patterns of uptake along the root axis and evaluation of the microelectrode flux estimation technique. Plant Physiology **99**, 734–747.

**Jackson MB, Drew MC.** 1984. Effects of flooding on growth and metabolism of herbaceous plants. In: Kozlowski TT, ed. Flooding and plant growth. New York: Academic Press, 47–128.

**Kulichikhin K, Yamauchi T, Watanabe K, Nakazono M.** 2014. Biochemical and molecular characterization of rice (*Oryza sativa* L.) roots forming a barrier to radial oxygen loss. Plant, Cell & Environment **37**, 2406–2420.

**Lin C, Sauter M.** 2018. Control of adventitious root architecture in rice by darkness, light, and gravity. Plant Physiology **176**, 1352–1364.

**Lorbiecke R, Sauter M.** 1999. Adventitious root growth and cell-cycle induction in deepwater rice. Plant Physiology **119**, 21–30.

**Loreti E, van Veen H, Perata P.** 2016. Plant responses to flooding stress. Current Opinion in Plant Biology **33**, 64–71.

**Malik AI, Islam AK, Colmer TD.** 2011. Transfer of the barrier to radial oxygen loss in roots of *Hordeum marinum* to wheat (*Triticum aestivum*): evaluation of four *H. marinum*–wheat amphiploids. New Phytologist **190**, 499–508.

**Mano Y, Omori F.** 2013. Flooding tolerance in interspecific introgression lines containing chromosome segments from teosinte (*Zea nicaraguensis*) in maize (*Zea mays* subsp. *mays*). Annals of Botany **112**, 1125–1139.

**Mori Y, Kurokawa Y, Koike M, Malik AI, Colmer TD, Ashikari M, Pedersen O, Nagai K.** 2019. Diel $O_2$ dynamics in partially and completely submerged deepwater rice: leaf gas films enhance internodal $O_2$ status, influence gene expression and accelerate stem elongation for 'snorkelling' during submergence. Plant & Cell Physiology **60**, 973–985.

**Olson KR, Lois WM.** 2017. Agricultural lands: flooding and levee breaches. In: Encyclopedia of soil science. CRC Press, 65–71.

**Pedersen O, Vos H, Colmer TD.** 2006. Oxygen dynamics during submergence in the halophytic stem succulent *Halosarcia pergranulata*. Plant, Cell & Environment **29**, 1388–1399.

**Pedersen O, Perata P, Voesenek LACJ.** 2017. Flooding and low oxygen responses in plants. Functional Plant Biology **44**, iii–ivi.

**Pedersen O, Sauter M, Colmer TD, Nakazono M.** 2020. Regulation of root adaptive anatomical and morphological traits during low soil oxygen. New Phytologist. doi: 10.1111/nph.16375.

**Phan-Van M, Rousseau D, De Pauw N.** 2008. Effects of fish bioturbation on the vertical distribution of water temperature and dissolved oxygen in a fish culture-integrated waste stabilization pond system in Vietnam. Aquaculture **281**, 28–33.

**Rich SM, Pedersen O, Ludwig M, Colmer TD.** 2013. Shoot atmospheric contact is of little importance to aeration of deeper portions of the wetland plant *Meionectes brownii*; submerged organs mainly acquire $O_2$ from the water column or produce it endogenously in underwater photosynthesis. Plant, Cell & Environment **36**, 213–223.

**Sauter M.** 2013. Root responses to flooding. Current Opinion in Plant Biology **16**, 282–286.

**Sasidharan R, Bailey-Serres J, Ashikari M, et al.** 2017. Community recommendations on terminology and procedures used in flooding and low oxygen stress research. New Phytologist **214**, 1403–1407.

**Setter TL, Kupkanchanakul T, Kupkanchanakul K, Bhekasut P, Wiengweera A, Greenway H.** 1987. Concentrations of $CO_2$ and $O_2$ in floodwater and in internodal lacunae of floating rice growing at 1–2 metre water depths. Plant, Cell & Environment **10**, 767–776.

**Shiono K, Yamauchi T, Yamazaki S, Mohanty B, Malik AI, Nagamura Y, Nishizawa NK, Tsutsumi N, Colmer TD, Nakazono M.** 2014. Microarray analysis of laser-microdissected tissues indicates the biosynthesis of suberin in the outer part of roots during formation of a barrier to radial oxygen loss in rice (*Oryza sativa*). Journal of Experimental Botany **65**, 4795–4806.

**Soukup A, Armstrong W, Schreiber L, Franke R, Votrubová O.** 2007. Apoplastic barriers to radial oxygen loss and solute penetration: a chemical and functional comparison of the exodermis of two wetland species, *Phragmites australis* and *Glyceria maxima*. New Phytologist **173**, 264–278.

**Steffens B, Geske T, Sauter M.** 2011. Aerenchyma formation in the rice stem and its promotion by $H_2O_2$. New Phytologist **190**, 369–378.

**Stünzi JT, Kende H.** 1989. Gas composition in the internal air spaces of deepwater rice in relation to growth induced by submergence. Plant & Cell Physiology **30**, 49–56.

**Tarlock AD, Chizewer DM.** 2016. Living with water in a climate-changed world: will federal flood policy sink or swim. Environmental Law **46**, 491.

**Watanabe K, Nishiuchi S, Kulichikhin K, Nakazono M.** 2013. Does suberin accumulation in plant roots contribute to waterlogging tolerance? Frontiers in Plant Science **4**, 178.

**Watanabe K, Takahashi H, Sato S, Nishiuchi S, Omori F, Malik AI, Colmer TD, Mano Y, Nakazono M.** 2017. A major locus involved in the formation of the radial oxygen loss barrier in adventitious roots of teosinte *Zea nicaraguensis* is located on the short-arm of chromosome 3. Plant, Cell & Environment **40**, 304–316.

**Yamaji N, Ma JF.** 2014. The node, a hub for mineral nutrient distribution in graminaceous plants. Trends in Plant Science **19**, 556–563.

**Yamauchi T, Colmer TD, Pedersen O, Nakazono M.** 2018. Regulation of root traits for internal aeration and tolerance to soil waterlogging–flooding stress. Plant Physiology **176**, 1118–1130.

**Yamauchi T, Shimamura S, Nakazono M, Mochizuki T.** 2013. Aerenchyma formation in crop species: a review. Field Crops Research **152**, 8–16.

**Yamauchi T, Tanaka A, Inahashi H, Nishizawa NK, Tsutsumi N, Inukai Y, Nakazono M.** 2019. Fine control of aerenchyma and lateral root development through AUX/IAA- and ARF-dependent auxin signaling. Proceedings of the National Academy of Sciences, USA **116**, 20770–20775.

**Yamauchi T, Yoshioka M, Fukazawa A, Mori H, Nishizawa NK, Tsutsumi N, Yoshioka H, Nakazono M.** 2017. An NADPH oxidase RBOH functions in rice roots during lysigenous aerenchyma formation under oxygen-deficient conditions. The Plant Cell **29**, 775–790.

**Zhang Q, Huber H, Boerakker JWT, Bosch D, de Kroon H, Visser EJW.** 2017. Environmental factors constraining adventitious root formation during flooding of *Solanum dulcamara*. Functional Plant Biology **44**, 858–866.

**Zhang X, Shabala S, Koutoulis A, Shabala L, Johnson P, Hayes D, Nichols DS, Zhou M.** 2015. Waterlogging tolerance in barley is associated with faster aerenchyma formation in adventitious roots. Plant and Soil **394**, 355–372.